TECHNICAL RESEARCH REPORT

Nonlinear Analysis of a High-Resolution Optical Wave-Front Control System

by E.W. Justh, P.S. Krishnaprasad, M.A. Vorontsov

CDCSS TR 2001-3
(ISR TR 2001-6)

The Center for Dynamics and Control of Smart Structures (CDCSS) is a joint Harvard University, Boston University, University of Maryland center, supported by the Army Research Office under the ODDR&E MURI97 Program Grant No. DAAG55-97-1-0114 (through Harvard University). This document is a technical report in the CDCSS series originating at the University of Maryland.

Web site http://www.isr.umd.edu/CDCSS/cdcss.html

Nonlinear analysis of a high-resolution optical wave-front control system

E.W. Justh and P.S. Krishnaprasad
Institute for Systems Research & ECE Dept.
University of Maryland
College Park, MD 20742
justh@isr.umd.edu, krishna@isr.umd.edu

M. A. Vorontsov
Intelligent Optics Laboratory
U.S. Army Research Laboratory
Adelphi, MD 20783
vorontsov@iol.arl.mil

Abstract

A class of feedback systems for high-resolution optical wave-front control (or adaptive optic wave-front distortion suppression) is modeled and analyzed. Under certain conditions, the nonlinear dynamical system models obtained are shown to be gradient systems, with energy functions that also serve as Lyapunov functions. The approach taken here to a problem of nonlinear control system design and analysis might also be applicable to other problems involving high-resolution control of physical fields, particularly if the field sensing is performed optically.

1 Introduction

The idea of using sensor and actuator arrays to manipulate physical fields is most developed in the area of adaptive optics (i.e., feedback control for optical wave-front phase distortion suppression). Cameras serve as sensor arrays, and spatial light modulators, such as liquid-crystal or MEMS micro-mirror devices, provide the actuation for manipulating optical beams. The control problem involves determining how the sensor and actuator arrays should be deployed, in addition to coordinating their activity. We consider the regime in which there are enough actuators and sensors that centralized control laws are impractical, and parallel, distributed processing is the only feasible approach. In high-resolution adaptive optic wave-front correction for atmospheric turbulence, stronger turbulence demands both higher actuator array resolution and faster speed of response. Therefore, centralized processing will always be ruled out at some strength of turbulence.

Correcting for the effects of atmospheric turbulence in laser communications, laser radar, imaging systems, and astronomy is one important application area for high-resolution wave-front control systems. Such systems could also potentially be used to monitor airflow and turbulence, e.g., for designing active aircraft surfaces. In addition, optical phase provides a mechanism for observing transparent objects other than atmospheric turbulence: the phase-contrast microscope is a well-known tool for imaging transparent biological specimens. Optical phase measurement is also useful for characterizing the surface topography of MEMS devices, e.g., the flatness of micro-mirror elements [1].

From a design and analysis standpoint, the challenge in using optical phase as a field quantity in a control system is that it introduces nonlinearity. Furthermore, even though the solution of interest is an equilibrium for the dynamical systems we consider, we are mainly interested in how the system behaves far from that equilibrium. The goal of the analysis is to capture the physics with sufficient fidelity, while keeping the nonlinear modeling simple enough to extract qualitative insights beyond what a linearized approximation to the dynamics can provide. This approach is prominent in the literature on spatio-temporal pattern-forming systems [2]. The analytical results also show how to design a wave-front control system which is actually a gradient system.

In section 2, we review conventional phase-contrast sensing, and describe Fourier phase filtering using SLMs. A block diagram of the wave-front control system is also presented. In section 3, we introduce the basic mathematical models, and in section 4 we present results for the model feedback system. The relationship of the analytical results to recent experimental work is discussed in section 5, with conclusions following in section 6.

This research was supported in part by grants from the Army Research Office under the ODDR&E MURI97 Program Grant No. DAAG55-97-1-0114 to the Center for Dynamics and Control of Smart Structures (through Harvard University), and by the National Science Foundation under the Learning and Intelligent Systems Initiative Grant CMS 9720334.

2 Phase-contrast wave-front sensing

Phase-contrast techniques date back to the Nobel-Prize-winning work of Frits Zernike during the 1930s [3]. The phase-contrast technique of Zernike can be understood in terms of the Fourier-transforming property of lenses, which is one manifestation of optical diffraction [4]. Assume a monochromatic input beam, so that it can be described using a complex envelope representation. As shown in figure 1, one lens Fourier-transforms the input beam, and the Zernike phase-plate (a glass slide with a phase-shifting dot perfectly centered on the optical axis) phase shifts the zero-order Fourier component relative to the rest of the Fourier spectrum. Another lens (or the same lens if the Zernike phase plate is reflective) then performs an inverse Fourier transform. The two parts of the beam with different Fourier-domain phase shifts then interfere to produce an intensity pattern which is a nonlinear measurement of the input beam phase. The nonlinearity is analogous to the sinusoidal nonlinearity of an interferometer, but in addition, there is nonlocal coupling arising from the fact that the "reference beam" is taken from the input beam. We refer to the system of figure 1 as the "conventional Zernike filter."

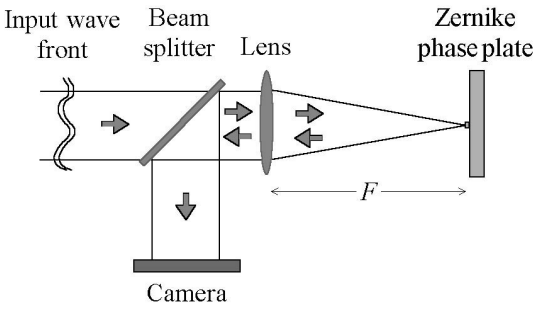

Figure 1: Zernike phase-contrast wave-front sensor.

A linearized description of (an idealized approximation to) the conventional Zernike filter, valid for small-magnitude phase variations in the input beam, was used by Zernike (in the context of microscopy) and by later authors (in the context of adaptive optics for astronomy) [5, 6]. The advantages of replacing the Zernike phase plate with an SLM have led to more recent interest in phase-contrast wave-front sensing [7-11].

If the input beam has a uniform intensity distribution over its cross-section, the linearized conventional Zernike filter output intensity distribution is the sum of a constant term and a term proportional to the input beam phase distribution. Although this suggests that the conventional Zernike filter might be suitable for parallel, distributed high-resolution feedback control, there are some practical difficulties. A block diagram of a wave-front corrector using a more general Fourier phase filter to overcome the limitations of the conventional Zernike filter is shown in figure 2, and it is assumed that both cameras have the same resolution and aspect ratio as their respective SLMs.

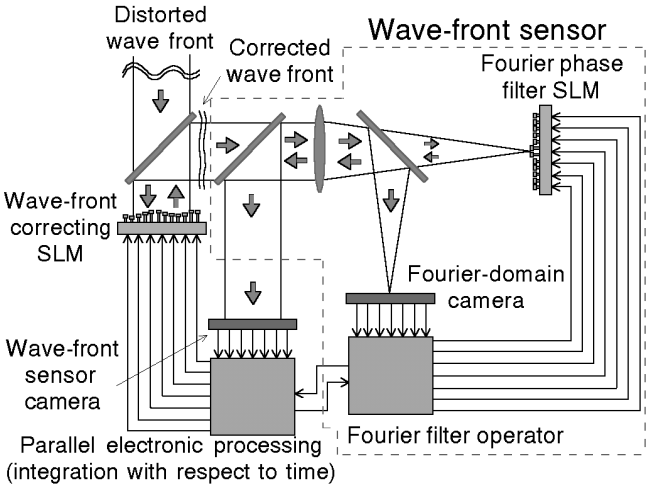

Figure 2: Feedback system with Fourier phase filter.

In figure 2, the input beam entering the system has an arbitrary wave-front phase distribution over its cross-section (which for simplicity we will assume to be static, but in general would be time-varying). The purpose of the phase-correcting SLM is to supply a complimentary phase-shift distribution to the input beam so that the corrected beam phase is spatially uniform. A portion of the corrected beam is sent to the Fourier phase filter, producing an intensity distribution which is recorded by the camera interfaced to the wave-front correcting SLM. Within the wave-front sensor, there is a second SLM and camera, which serves as a time-varying Fourier phase filter (with the Fourier-domain phase-shift distribution dependent on the Fourier-domain intensity distribution of the corrected beam). The system of figure 2 is thus nonlinear, has hundreds of thousands (potentially millions) of degrees of freedom, and has interactions between the Fourier-filtering operation and the phase-correction dynamics.

Analysis of the mathematical models described in the next section for the system of figure 2 reveals that a "differential" approach yields gradient dynamical systems. The differential approach involves alternating between one Fourier phase filter distribution, and the corresponding negative Fourier phase filter distribution. The resulting Fourier-filter output intensity distributions are then differenced to produce the image which is integrated with respect to time and fed back to the phase-correcting SLM.

As phase-correction proceeds, and the Fourier filter changes, the energy functional for gradient dynamics may also change. By understanding the gradient dynamics behavior for a fixed Fourier filter, and understanding how the Fourier filter will evolve as phase-

correction proceeds, it should be possible to obtain convergence results for specific choices of the Fourier filter operator (i.e., the dependence of the Fourier phase filter upon the Fourier-domain intensity measurement). For simplicity, and to bring out the main ideas, we focus here on the gradient dynamics behavior for fixed choices of the Fourier phase filter, starting with the differential version of the conventional Zernike filter.

3 Mathematical models

To describe the optical field (for a monochromatic beam), we introduce a complex envelope $A(x, y, z)$, describing a single component of the electric or magnetic field. We distinguish the z direction as the "optical axis," and denote the transverse coordinates as $\mathbf{r} = (x, y)$. The underlying electromagnetic field component that $A(\mathbf{r}, z)$ represents is then obtained by taking the real part of $A(\mathbf{r}, z)\mathrm{e}^{i(\omega t - kz)}$, where $k = 2\pi/\lambda$ and $\omega = kc$ (with λ the optical wavelength, and c the speed of light).

The complex envelope $A(\mathbf{r}, z)$ can be expressed in polar form as

$$A(\mathbf{r}, z) = a(\mathbf{r}, z)\mathrm{e}^{iu(\mathbf{r},z)}, \tag{1}$$

where $[a(\mathbf{r}, z)]^2$ is the intensity and $u(\mathbf{r}, z)$ is the phase (the quantity we are interested in measuring and controlling). The intensity is what a camera would measure at the point z along the optical axis.

In the wave-front control setting, we are interested in how the phase at a particular point z_0 along the optical axis evolves in time. Therefore, we drop the argument z from equation (1), and we allow u to depend on a time variable t. (This time variable corresponds to quasi-static changes in the complex envelope, not the time scale of electromagnetic field oscillations.)

3.1 Wave-front sensor model

Our Zernike filter model should phase-shift the zero-order Fourier component of the complex envelope $a(\mathbf{r})\mathrm{e}^{iu(\mathbf{r},t)}$ by θ (ideally, $\theta = \pi/2$, but we only require $0 < \theta < \pi$), relative to the rest of the Fourier spectrum. Therefore, we need to formulate mathematically what we mean by the "zero-order Fourier component." Because we assume that $a(\mathbf{r}) = 0$ outside of a bounded region, we can use a Fourier series representation:

$$\begin{aligned} A(\mathbf{r}, t) &= \sum_{\mathbf{p}} \mathrm{a}_{\mathbf{p}}(t)\mathrm{e}^{i\frac{2\pi}{\gamma}\mathbf{p}\cdot\mathbf{r}}, \\ \mathrm{a}_{\mathbf{p}}(t) &= \frac{1}{\gamma^2}\int A(\mathbf{r}, t)\mathrm{e}^{-i\frac{2\pi}{\gamma}\mathbf{p}\cdot\mathbf{r}}d\mathbf{r}, \end{aligned} \tag{2}$$

where $\mathbf{p}$ is a pair of integers (each ranging from $-\infty$ to ∞), and γ is a parameter determining the spectral resolution (assumed sufficiently large to avoid aliasing).

We model the conventional Zernike filter as an operator $f_{conv}(u)$ which takes a phase distribution $u(\mathbf{r}, t)$ at the Zernike filter input and maps it to an intensity distribution $[f_{conv}(u)](\mathbf{r}, t)$ at the Zernike filter output. This operator should correspond to phase-shifting the zero-order Fourier series component by θ, and then taking the intensity (i.e., the magnitude) of the resulting complex envelope. We thus obtain

$$\begin{aligned} &[f_{conv}(u)](\mathbf{r}, t) \\ &\quad = \left| a(\mathbf{r})\mathrm{e}^{iu(\mathbf{r},t)} + (\mathrm{e}^{i\theta} - 1)\frac{1}{\gamma^2}\int a(\mathbf{r})\mathrm{e}^{iu(\mathbf{r},t)}d\mathbf{r}\right|^2. \end{aligned} \tag{3}$$

(We have ignored finite aperature effects by failing to truncate the Fourier series at some finite frequency.) The corresponding differential Zernike filter model is

$$\begin{aligned} &[f_{diff}(u)](\mathbf{r}, t) \\ &\quad = \left| a(\mathbf{r})\mathrm{e}^{iu(\mathbf{r},t)} + (\mathrm{e}^{i\theta} - 1)\frac{1}{\gamma^2}\int a(\mathbf{r})\mathrm{e}^{iu(\mathbf{r},t)}d\mathbf{r}\right|^2 \\ &\quad\quad - \left| a(\mathbf{r})\mathrm{e}^{iu(\mathbf{r},t)} + (\mathrm{e}^{-i\theta} - 1)\frac{1}{\gamma^2}\int a(\mathbf{r})\mathrm{e}^{iu(\mathbf{r},t)}d\mathbf{r}\right|^2 \\ &\quad = -4\sin\theta\ \mathrm{Im}\left\{ a(\mathbf{r})\mathrm{e}^{-iu(\mathbf{r},t)}\frac{1}{\gamma^2}\int a(\mathbf{r})\mathrm{e}^{iu(\mathbf{r},t)}d\mathbf{r}\right\}. \end{aligned} \tag{4}$$

At each point $\mathbf{r}$, the output intensity is a periodic function of the input phase, but there is also global coupling though the zero-order Fourier component $(1/\gamma^2)\int a e^{iu}d\mathbf{r}$. Equation (4) also reveals that the wave-front sensor image contrast depends on the zero-order Fourier component, which has important practical implications.

3.2 Feedback system model

The feedback system using the differential Zernike filter model given by equation (4) is

$$\frac{\partial u}{\partial t} = -f_{diff}(u). \tag{5}$$

Since the phase-correcting SLM has finite resolution, we could instead consider a finite collection of ordinary differential equations as our model. However, the continuous formulation is notationally simpler, and makes it easier to add diffusion (or even diffraction) to the model.

The dynamics given by equation (5) are (formally) gradient dynamics with respect to the energy functional

$$[V(u)](t) = -2\gamma^2\sin\theta\left|\frac{1}{\gamma^2}\int a(\mathbf{r})\mathrm{e}^{iu(\mathbf{r},t)}d\mathbf{r}\right|^2, \tag{6}$$

which is proportional to (the negative of) the power in the zero-order Fourier component. Using variational calculus, we obtain

$$\frac{dV}{dt} = \frac{\delta V}{\delta u}\cdot\frac{\partial u}{\partial t} = -\int\left(\frac{\partial u}{\partial t}\right)^2 d\mathbf{r}, \tag{7}$$

where $(\delta V/\delta u)\cdot v = \lim_{\epsilon\to 0}[V(u+\epsilon v)-V(u)]/\epsilon$. The feedback system using the differential version of the conventional Zernike filter thus evolves to maximize the power in the zero-order Fourier component of the corrected beam. It is clear that $u(\mathbf{r},t)=u_0$, a uniform phase, minimizes $V(u)$, so that phase correction corresponds to energy functional minimization.

4 Results for the feedback system model

The gradient dynamics property of the differential Zernike filter feedback system is retained even when we add diffusion, phase-shift spectral components besides the zero-order component, and discretize the phase-correcting SLM. We will first explain each of these modifications individually, and then combine them into two propositions summarizing the gradient-flow behavior of these wave-front control systems. (The assumption of a monochromatic beam can also be relaxed, but that analysis is omitted here due to space constraints.)

4.1 Arbitrary Fourier phase filter

A feedback system based on the differential Zernike filter of equation (4) would suffer from the main practical problem associated with the conventional Zernike filter: too little power may fall on the pixel used for phase-shifting the zero-order Fourier component, and therefore the initial wave-front sensor image contrast may be too low for phase correction to begin. The point of measuring the Fourier-domain intensity distribution and using an SLM to implement the Fourier phase filter, as shown in figure 2, is to ensure that enough of the spectral power is phase-shifted to produce an image with sufficient contrast.

Consider first the case where an arbitrary collection of Fourier series components of the input beam complex envelope are phase shifted by the same amount θ. Equation (4) is then replaced by

$$\begin{aligned} f(u) = &\left| a\mathrm{e}^{iu} + \left(\mathrm{e}^{i\theta}-1\right)\sum_{\mathbf{p}\in I}\left(\frac{1}{\gamma^2}\int a\mathrm{e}^{iu}\mathrm{e}^{-i\frac{2\pi}{\gamma}\mathbf{p}\cdot\mathbf{r}}d\mathbf{r}\right)\mathrm{e}^{i\frac{2\pi}{\gamma}\mathbf{p}\cdot\mathbf{r}}\right|^2 \\ &- \left| a\mathrm{e}^{iu} + \left(\mathrm{e}^{-i\theta}-1\right)\sum_{\mathbf{p}\in I}\left(\frac{1}{\gamma^2}\int a\mathrm{e}^{iu}\mathrm{e}^{-i\frac{2\pi}{\gamma}\mathbf{p}\cdot\mathbf{r}}d\mathbf{r}\right)\mathrm{e}^{i\frac{2\pi}{\gamma}\mathbf{p}\cdot\mathbf{r}}\right|^2 \\ &= -4\sin\theta\sum_{\mathbf{p}\in I}\mathrm{Im}\left\{a\mathrm{e}^{-i(u-\frac{2\pi}{\gamma}\mathbf{p}\cdot\mathbf{r})}\frac{1}{\gamma^2}\int a\mathrm{e}^{i(u-\frac{2\pi}{\gamma}\mathbf{p}\cdot\mathbf{r})}d\mathbf{r}\right\}, \end{aligned} \tag{8}$$

where I is a finite index set that may or may not contain $\mathbf{0}$. As we will show, the gradient dynamics property holds for $f(u)$ given by equation (8).

One consequence is that the model is unaffected by which Fourier series component we consider to be the "zero-order" component. Suppose $I=\{\mathbf{p}_0\}$, i.e., exactly one arbitrarily chosen Fourier series component is phase-shifted. If we define $\tilde{u}=u-\frac{2\pi}{\gamma}\mathbf{p}_0\cdot\mathbf{r}$, then we have

$$f(u) = f_{diff}(\tilde{u}). \tag{9}$$

The dynamics then become

$$\frac{\partial\tilde{u}}{\partial t} = \frac{\partial u}{\partial t} = -f(u) = -f_{diff}(\tilde{u}). \tag{10}$$

Thus, $\tilde{u}$ evolves according to equation (5), but the spatially uniform equilibrium, $\tilde{u}_o\equiv 0$, actually corresponds to $u_o(\mathbf{r})=\frac{2\pi}{\gamma}\mathbf{p}_0\cdot\mathbf{r}$, a solution representing a pure wave-front "tilt." Equation (8) can also be used to study what happens when the spectral phase-shifting SLM is lower-resolution than the focused spot size of an unaberrated beam.

When the spectral phase shift distribution is arbitrary (rather than constrained to take the values 0 or θ for all Fourier series coefficients), the gradient dynamics property no longer holds for the differential Zernike filter. However, it is still instructive to examine the nonlinear dynamics (see section 5).

4.2 Diffusion added to the dynamics

Adding diffusion to the dynamics may be useful for penalizing phase jumps in the phase-correcting SLM. To analyze the dynamics with the diffusion term, it is necessary to distinguish between the input beam phase $\phi(\mathbf{r})$ and the phase-correcting SLM phase distribution $u(\mathbf{r},t)$, since the diffusion term only involves the latter. Equation (5) is thus replaced by

$$\frac{\partial u}{\partial t} = l^2\Delta u - f(u+\phi), \tag{11}$$

where $l>0$ is a diffusion length. Using standard methods from PDE theory (and assuming periodic boundary conditions consistent with our Fourier series representation), it is possible to prove existence and uniqueness of weak solutions for equation (11). The energy functionals we write down are therefore well-defined.

4.3 Discretized phase-correcting SLM

So far we have assumed a phase-correcting SLM with infinitely high resolution. It is useful to know what hypotheses are needed to derive analogous results for a more realistic model which assumes that the phase-correcting SLM is spatially discretized.

Let the wavefront correction element be described by

$$u(\mathbf{r},t) = S(\mathbf{r}, u_{11}(t), u_{12}(t)..., u_{nn}(t)), \tag{12}$$

where the $u_{ij}(t)$ are electrode voltages causing deformation of, say, a deformable mirror. A natural choice for a discrete approximation to equation (11), corresponding

to principal component analysis, is

$$\frac{du_{ij}}{dt} = l^2\left(\frac{u_{(i-1)j} + u_{i(j-1)} + u_{(i+1)j} + u_{i(j+1)} - 4u_{ij}}{\delta^2}\right) - \int \frac{\partial S}{\partial u_{ij}} f(S(\mathbf{r}, u_{11}, u_{12}, ..., u_{nn}) + \phi) d\mathbf{r}. \quad (13)$$

The parameter δ corresponds to the length scale of the spatial discretization of the wave-front corrector. (In a practical implementation, we would probably approximate the $\partial S/\partial u_{ij}$ as functions of $\mathbf{r}$ alone.)

From expression (13) for the dynamics, we see that it is not necessary to measure $f(u+\phi)$, only certain spatially weighted functionals of $f(u+\phi)$. Thus, as long as the response of an array of photodetectors is appropriately matched to a finite degree-of-freedom wavefront corrector, phase distortion suppression may be achievable. Furthermore, the photodetector signals could be directly fed back to the corresponding electrodes of the phase-correcting SLM, with the only computation required being the subtraction needed for the differential approach (and integration with respect to time).

4.4 Results for the differential Zernike filter

We present the main results for the differential Zernike filter model as two propositions. One applies to the continuous (PDE) system, and the other applies to the corresponding spatially discretized system of ODEs. Although the differential approach can only (practically) be implemented in discrete time, we leave time as a continuous variable in the propositions.

Proposition 1. Consider the dynamical system (11), and let $f(u)$ be given by equation (8). Assume the initial condition $u(\mathbf{r}, 0) \in L^2(\Omega)$ and $\phi(\mathbf{r}) \in L^2(\Omega)$ (where Ω is the bounded region corresponding to the periodic boundary conditions). Assume further that I is a finite set, $\int [a(\mathbf{r})]^2 d\mathbf{r}$ is bounded, and γ is sufficiently large to avoid aliasing. Then the dynamical system is a gradient system with respect to the energy functional

$$V = \int \frac{l^2}{2} |\nabla u|^2 d\mathbf{r} - 2\gamma^2 \sin\theta \sum_{\mathbf{p}\in I} \left| \frac{1}{\gamma^2} \int a(\mathbf{r}) \mathrm{e}^{i(u(\mathbf{r},t) + \phi(\mathbf{r}) - \frac{2\pi}{\gamma}\mathbf{p}\cdot\mathbf{r})} d\mathbf{r} \right|^2. \quad (14)$$

Specifically, $\partial u/\partial t = -\nabla V$ (with respect to the usual inner product for $L^2(\Omega)$), and

$$\frac{dV}{dt} = -\int \left(\frac{\partial u}{\partial t}\right)^2 d\mathbf{r}. \quad (15)$$

Thus, V also serves as a Lyapunov functional for the dynamics; i.e., $dV/dt \leq 0$, with $dV/dt = 0$ only at equilibria.

Proof: From equation (8) and our assumptions on a and I, we have

$$\int [f(u)]^2 d\mathbf{r} < c_1 < \infty, \ \ \forall u. \quad (16)$$

Therefore, equation (11) has a unique solution with sufficient regularity for the subsequent calculations [12].

Differentiating the energy functional V with respect to time gives

$$\frac{dV}{dt} = \frac{\delta V}{\delta u} \cdot \frac{\partial u}{\partial t} = -\int \left(\frac{\partial u}{\partial t}\right)^2 d\mathbf{r}. \quad (17)$$

This calculation shows that $\partial u/\partial t = -\nabla V$, and that $dV/dt \leq 0$ with $dV/dt = 0$ only at equilibria. □

Proposition 2. Let the driving voltages for an n^2 degree-of-freedom phase-correcting SLM be denoted $u_{ij}(t)$, and let $S(\mathbf{r}, u_{11}, u_{12}, ..., u_{nn})$ be a smooth function (representing the SLM influence function). Consider the dynamical system given by equation (13), where $u_{ij} = 0$ when either i or j is outside the range from 1 to n. As before, we assume that I is a finite set, $\int [a(\mathbf{r})]^2 d\mathbf{r}$ is bounded, and γ is sufficiently large to avoid aliasing. We also assume that

$$\int \left(\frac{\partial S}{\partial u_{ij}}\right)^2 d\mathbf{r} < c_2 < \infty, \quad (18)$$

for each i, j between 1 and n, and that the right-hand-side of equation (13) is continuously differentiable with respect to $u_{11}, u_{12}, ..., u_{nn}$. Then the dynamical system (13) is a gradient system with respect to the energy function V_δ given by

$$V_\delta = \frac{l^2}{\delta} \sum_{i=1}^{n} \sum_{j=1}^{n} \left(2(u_{ij})^2 - u_{(i-1)j}u_{ij} - u_{i(j-1)}u_{ij}\right) - 2\gamma^2 \sin\theta \sum_{\mathbf{p}\in I} \left| \frac{1}{\gamma^2} \int a(\mathbf{r}) \mathrm{e}^{i(S(\mathbf{r},u_{11},...,u_{nn}) + \phi - \frac{2\pi}{\gamma}\mathbf{p}\cdot\mathbf{r})} d\mathbf{r} \right|^2. \quad (19)$$

Specifically, $du_{ij}/dt = -\partial V_\delta/\partial u_{ij}$, and

$$\frac{dV_\delta}{dt} = -\sum_{i=1}^{n} \sum_{j=1}^{n} \left(\frac{du_{ij}}{dt}\right)^2. \quad (20)$$

Thus, V_δ also serves as a Lyapunov function for the dynamics; i.e., $dV_\delta/dt \leq 0$, with $dV_\delta/dt = 0$ only at equilibria.

Proof: Equation (16) is valid, because $f(u)$ is the same as in Proposition 1. It then follows that for any initial condition, equation (13) has a unique solution, defined for t arbitrarily large (i.e., the necessary local Lipschitz condition is satisfied, and finite escape times are ruled out) [13].

Differentiating the energy function V_δ with respect to time gives

$$\frac{dV_\delta}{dt} = \sum_{i=1}^{n}\sum_{j=1}^{n} \frac{\partial V_\delta}{\partial u_{ij}} \frac{du_{ij}}{dt} = -\sum_{i=1}^{n}\sum_{j=1}^{n} \left(\frac{du_{ij}}{dt}\right)^2 . \quad (21)$$

This calculation shows that $du_{ij}/dt = -\partial V_\delta/\partial u_{ij}$, and that $dV_\delta/dt \leq 0$ with $dV_\delta/dt = 0$ only at equilibria. □

5 Relationship to experimental work

The preceeding analysis shows how a wave-front control system can be designed so as to be a gradient dynamical system. What is required is to use the differential approach for wave-front sensing, and have the Fourier phase filter supply phase shifts of exactly 0 or θ. However, in numerical and experimental work, fairly robust convergence has been observed, even when these conditions are relaxed (provided the Fourier-domain phase shifts remain between 0 and π) [11]. We can thus use the gradient dynamical system as a nonlinear approximation to these non-gradient systems, and this type of approximation appears to have greater qualitative value than a linearized approximation about the spatially uniform equilibrium.

In recent experimental work, the system of figure 2 was implemented with a liquid-crystal light valve (LCLV) used as the Fourier phase filter [11]. The LCLV device supplied a phase shift proportional to incident optical intensity. For our Fourier series model, the operator corresponding to the LCLV would have each Fourier series component phase-shifted in proportion to its intensity. The differential approach was not used, as the LCLV could only supply phase shifts of one polarity. For uniform-intensity input beams, the LCLV-based system performed quite well (both in simulation and experimentally), correcting input beams with highly-aberrated phase distributions. Performance degraded with increasing variation in the input beam intensity distribution (which is reasonable, since in that case perfect phase correction no longer corresponds to an equilibrium of the dynamics) [11].

6 Summary and conclusions

Large arrays of sensors and actuators are becoming feasible to build. However, using such arrays for feedback control of physical fields depends critically on our ability to devise control schemes for such systems. Optics is a natural context in which to investigate such control schemes, because there has been considerable work in adaptive optics to draw upon, and because optics can be useful for measurement in other engineering contexts, as well.

However, in considering optical wave-front measurement and control, nonlinearity enters in an intrinsic way. We need to be able to deal with the nonlinearity, as well as with the constraints arising from having to use a parallel, distributed control scheme rather than a centralized control law. The strategy of identifying a nonlinear approximation to the dynamics which captures its essential features even far from equilibrium can be simpler to carry out, and more revealing, than a linearized analysis about the equilibrium. Furthermore, the results can be used to guide design.

References

[1] *SPIE Proceedings, Phase Contrast and Differential Interference Contrast Imaging Techniques and Applications,* Vol. 1846, 1994.

[2] M.C. Cross and P.C. Hohenberg, "Pattern formation outside of equilibrium," *Reviews of Modern Physics,* Vol. 65, No. 3, pp. 851-1112, 1993.

[3] F. Zernike, "How I Discovered Phase Contrast," *Science*, Vol. 121, pp. 345-349, 1955.

[4] J.W. Goodman, *Introduction to Fourier Optics*, McGraw-Hill, New York, 1996.

[5] John W. Hardy, "Active Optics: A New Technology for the Control of Light," *Proceedings of the IEEE*, Vol. 66, No. 6, pp. 651-697, 1978.

[6] R.H. Dicke, "Phase-contrast detection of telescope seeing errors and their correction," *The Astrophysical Journal,* Vol. 198, pp. 605-615, 1975.

[7] V.Yu. Ivanov, V.P. Sivokon, and M.A. Vorontsov, "Phase retrieval from a set of intensity measurements: theory and experiment," *J. Opt. Soc. Am. A*, Vol. 9, No. 9, pp. 1515-1524, 1992.

[8] J. Glückstad, "Adaptive array illumination and structured light generated by spatial zero-order self-phase modulation in a Kerr medium," *Optics Communications*, Vol. 120, pp. 194-203, 1995.

[9] A. Seward, F. Lacombe, and M. K. Giles, "Focal plane masks in adaptive optics systems," *SPIE Proceedings*, Vol. 3762, pp. 283-293, July 1999.

[10] M.A. Vorontsov, E.W. Justh, and L.A. Beresnev, "Adaptive Optics with Advanced Phase Contrast Techniques, Part I: High-Resolution Wavefront Sensing," submitted to *J. Opt. Soc. Am. A*, 2000.

[11] E.W. Justh, M.A. Vorontsov, G. Carhart, L.A. Beresnev, and P.S. Krishnapasad, "Adaptive Optics with Advanced Phase Contrast Techniques, Part II: High-Resolution Wavefront Control," submitted to *J. Opt. Soc. Am. A*, 2000.

[12] Lawrence Evans. *Partial Differential Equations.* American Mathematical Society, Providence, 1998.

[13] H. Khalil. *Nonlinear Systems.* New York: Macmillan Publishing Co., 1992.